VOLTAGE CLAMP OF THE EARTHWORM SEPTUM

V. VERSELIS AND P. R. BRINK
Department of Anatomical Sciences, State University of New York at Stony Brook, Stony Brook, New York 11794

The septal membranes between the cells that comprise the earthworm median giant axon contain low-resistance junctions (nexus) capable of transmitting current flow sufficient to allow propagation of action potentials between cells (1). These junctions are morphologically classified as A-type (2). When using coupling ratio and transfer resistance measurements to monitor junctional membrane resistance (r_j), the low values for r_j are masked by the dominant nonjunctional resistance component of the transfer resistance, making potentially significant changes in r_j difficult to detect (3, 4). In the present study, we applied a more sensitive technique, utilizing voltage-clamp to see if subtle changes in r_j could be measured. In particular, the effects of transjunctional voltage and altered cytoplasmic pH were investigated. With this preparation, favorable geometry minimizes difficulties in quantitatively estimating r_j that arise from current flow through nonjunctional membrane pathways and complex coupling topologies. A modified voltage-clamp adopted from Johnston and Ramon (5) provided precise control of transjunctional potential.

MATERIALS AND METHODS

In each experiment, four low-resistance microelectrodes (5–10 MΩ), one for passing current, two for differential voltage recording, and one to provide a reference ground, were inserted as depicted in Fig. 1. The external bath was left floating and all potentials were referenced to the internal ground electrode. TTX (1×10^{-7} M) and TEA (1×10^{-6} M) were added to the bath solution to abolish excitation of the plasma membrane. The steady-state spatial profile of transmembrane voltage was derived by treating a short stretch of axon as a one-dimensional, finite cable (length $2L$) terminated at both ends by an infinite resistance (1, 6). The cable endpoints, L and $-L$, refer to the location of the current-passing and ground electrodes. Centered between these two electrodes, at $x = 0$, the internal axial pathway is connected by a junctional resistance, r_j, insulated from the extracellular space. The equations that describe the steady-state transmembrane potential (V_m) and internal axial current (I_i) as a function of distance, x, are

$$V_m(x) = -\lambda r_i I_p \left[\frac{r_j \cosh(x/\lambda) - \lambda r_i \sinh(x/\lambda)}{r_j \sinh(L/\lambda) + \lambda r_i \cosh(L/\lambda)}\right] \quad \text{for } -L \le x \le 0 \quad (1)$$

$$V_m(x) = \lambda r_i I_p \left[\frac{r_j \cosh(x/\lambda) + \lambda r_i \sinh(x/\lambda)}{r_j \sinh(L/\lambda) + \lambda r_i \cosh(L/\lambda)}\right] \quad \text{for } 0 \le x \le L \quad (2)$$

$$I_i(x) = -I_p \left[\frac{r_j \sinh(x/\lambda) - \lambda r_i \cosh(x/\lambda)}{r_j \sinh(L/\lambda) + \lambda r_i \cosh(L/\lambda)}\right] \quad \text{for } -L \le x \le 0 \quad (3)$$

$$I_i(x) = I_p \left[\frac{r_j \sinh(x/\lambda)\,\rho + \cosh(x/\lambda)}{r_j \sinh(L/\lambda) + \lambda r_i \cosh(L/\lambda)}\right] \quad \text{for } 0 \le x \le L \quad (4)$$

where r_j = junctional resistance (Ω), r_a = axoplasmic resistance (Ω/cm), λ = space constant (cm), and I_p = applied internal current (namps).

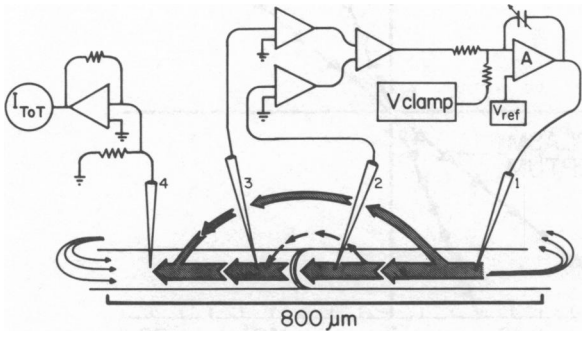

FIGURE 1. Diagram of the experimental arrangement. Four electrodes are inserted into the "axon," two in each cell. The distance between the stimulating and ground electrodes is typically under 1 mm. The difference voltage across the junction (electrodes #2 and #3) is compared to a clamp voltage at the summing pole of a differential operational amplifier (A). The amplified output (10^4) is applied to the current-passing electrode (#1). A current monitor in the ground line (electrode #4) provided a measure of the total current. Arrows represent the direction and magnitude of current flow.

RESULTS AND DISCUSSION

The steady-state profiles of transmembrane voltage and internal longitudinal current derived from cable theory are depicted in Fig. 2. When the length of axon between $-L$ and L is kept short relative to the space constant, most of the internally applied current flows longitudinally down the axon core with little or no transmembrane current (Fig. 2 *B*). The solid lines represent theoretical curves with r_j values of 0, 30, and 300 KΩ. The measured values agree well with the theoretical predictions, indicating that the finite cable analogy is a fairly good approximation of the actual experimental condition, even though the axon extends beyond $x = -L$ and $x = L$ (Fig. 1). Current flow in this extrapolar pathway is small (<10%) and will not be considered. With larger junctional resistances, more current is shunted across the plasma membrane, resulting in larger values for V_m. In fact, 50% of the applied current will be shunted across the membrane when r_j approximates the input resistance of the cell (1,000 kΩ). However, since r_j is small relative to the input resistance, nonjunctional currents are minimal. A direct measure of the internal longitudinal resistance can be made by dividing the internal longitudinal voltage drop by the applied current ($r_i = \Delta V_i / I_p$). Resistance measurements were also made in

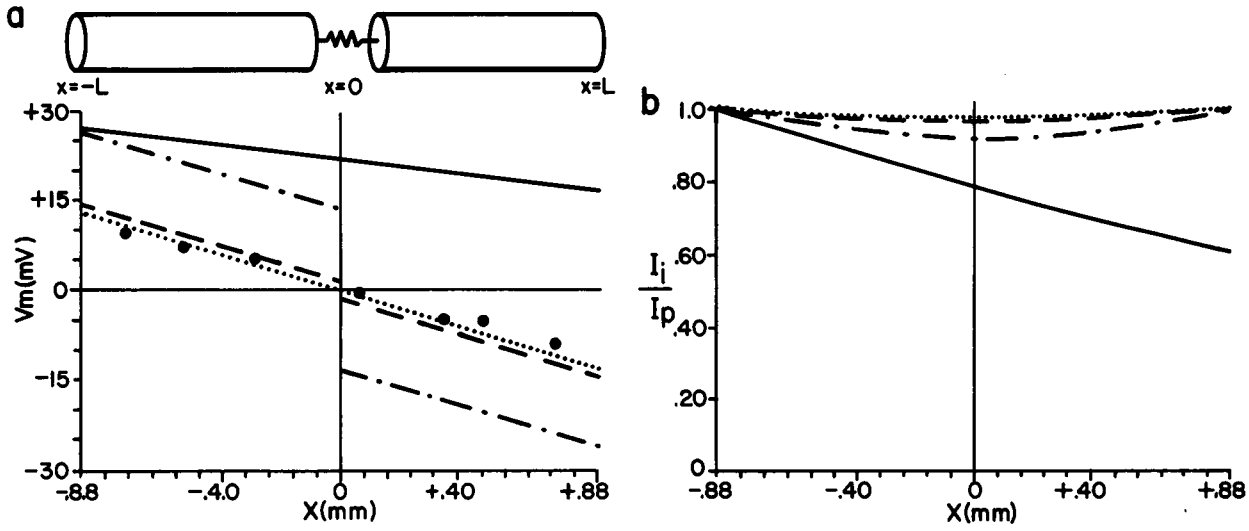

FIGURE 2 *A*, steady-state transmembrane potential as a function of distance. Values for r_j and λ were obtained at the beginning of the experiment ($I_p = -50$ nA). These values were used to obtain theoretical curves for $V_m(x)$ using Eqs. 1 and 2 with r_j values of 0 KΩ (· · ·), 30 kΩ (---) and 300 kΩ (-·-·-). •'s represent actual data points. For comparison, $V_m(x)$ is plotted for the semi-infinite cable, $x \rightarrow +\infty$, with an external ground (—). *B*, steady-state longitudinal current as a function of distance (Eqs. 3 and 4) with r_j values as in *A*. The ordinate is plotted as the percentage of the total current that is applied ($I_i(x)/I_p$), where $I_i(x = L) = I_p$. Note that a large percentage of the total current flows internally, especially with small values for r_j.

regions of axoplasm that did not contain septa in order that the junctional resistance component could be extracted from the longitudinal resistance term r_i, where $r_i = (r_j + r_a)$. To distinguish the septa, axons were injected with dye after electrical measurements were completed. Compared to axoplasmic resistance measurements the presence of a septum always resulted in a detectably larger resistance value. The average junctional resistance was calculated to be 30–50 kΩ.

An additional advantage of this internal-ground technique is that large internal current densities can be applied without damaging the plasma membrane because little

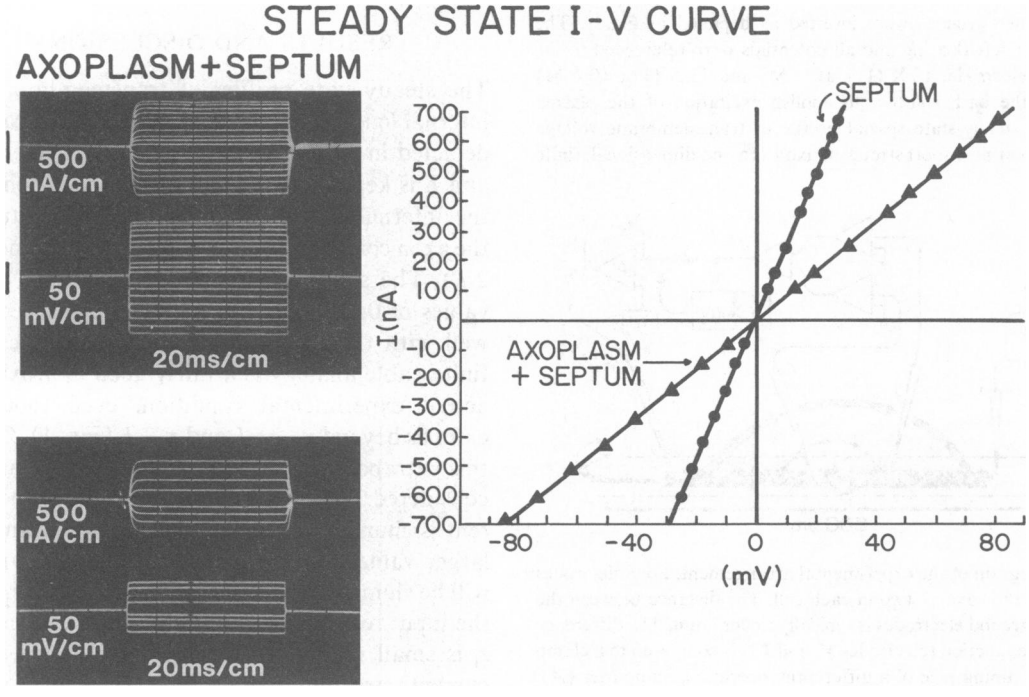

FIGURE 3 Steady-state current-voltage relationship for the septum. The values were obtained from the set of records shown. The voltage across the septal membrane was obtained by subtracting away the voltage drop caused by the series resistance due to axoplasm (*bottom* records) from the total voltage drop across septum plus axoplasm (*top* records).

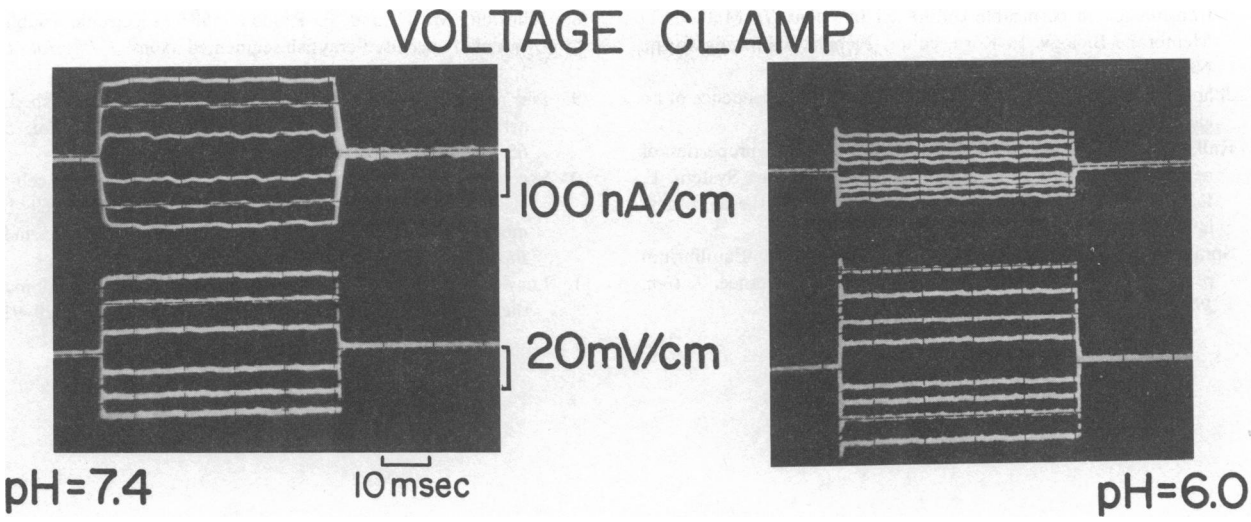

FIGURE 4 Effect of pH on junctional resistance. Records of a series of current and voltage steps (voltage clamp) at pH 7.4 and pH 6.0.

current flows across it. This is evident from the smaller magnitude of the transmembrane potential V_m ($-L$) at the point of injection compared to the infinite cable case (Fig. 2 *A*). The inherently low resistance of the junctional membranes in series with the axoplasmic resistance necessitates large current densities in order to achieve a substantial voltage drop (V_j) across the junctional membrane. This is important because the threshold value for the onset of voltage dependence in A-type junctions from adult tissue may occur at higher tranjunctional voltages than in amphibian blastomeres, where junctional conductance increases when V_j exceeds 10–15 mV (7).

Fig. 3 demonstrates the *I-V* characteristics of the junctional membranes under voltage clamp. The steady state *I-V* curve was found to be linear in the range ±30 mV after series resistance due to axoplasm was taken into consideration. Transjunctional voltages up to 50 mV did not alter the ohmic *I-V* relationship. Slow time constants for uncoupling were not seen even with voltage steps of long duration (up to 5 s). Similar voltage independence was demonstrated in perfused crayfish lateral giant axons (8) that contain B-type junctions (9). It is interesting to note that these perfused junctions were also insensitive to changes in axoplasmic pH and elevated Ca^{++} concentrations.

To determine whether the earthworm septal membranes are resistant to uncoupling, the intracellular pH was altered by soaking the nerve cord in an acetate-buffered saline at pH 6.0. Within 15–20 minutes, r_j increased an average of 10-fold (300–400 kΩ, Fig. 4). The effects of pH were partially reversible (80% recovery) when the pH was raised back to 7.4. Identical experiments done in regions containing only axoplasm showed no change in resistance, indicating that this phenomenon is associated with the junctional membranes. Because the cells depolarized substantially with pH, the experiments were done in high external potassium (70 mM) as a control. No change in resistance could be detected. This suggests that the increase in r_j is pH-related and not related to transjunctional or cell membrane potential (10). Even though the resistance of the junctional membranes increased substantially, a large residual conductance still exists in this "uncoupled" state. Can these cells be considered to be functionally uncoupled; that is, can action potentials still propagate from cell to cell? This could not be investigated, because lowering the pH rendered these cells incapable of generating an action potential.

These results raise interesting questions about modulation of junctional conductance. Do Ca^{++}, pH, and voltage act on the same site? We have demonstrated that the junctions between the cells that comprise the median giant axon do not possess voltage-sensitive gates, yet they are sensitive to pH. Whether the 10-fold increase in junctional resistance is physiologically relevent remains to be seen. A great deal of variability exists in the degree of uncoupling among tissue types exposed to similar experimental conditions (11). Much of this variability can result from differences in cytoplasmic buffering capacity among cell types. From a teleological point of view, channel heterogeneity among tissue types is a strong possibility when structure-function relationships are considered.

This work was supported by a National Institutes of Health grant GM 24905.

Received for publication 29 April 1983.

REFERENCES

1. Brink, P. R., and L. Barr. 1977. The resistance of the septum of the median giant axon of the earthworm. *J. Gen. Physiol.* 69:517–536.
2. Brink, P. R., and M. M. Dewey. 1978. Nexal membrane permeability to anions. *J. Gen. Physiol.* 72:62–86.
3. Bennett, M. V. L. 1966. Physiology of electrotonic junctions. *Ann. NY Acad. Sci.* 137:509–539.
4. Socolar, S. J., and W. R. Loewenstein. 1979. Methods for studying

transmission in permeable cell-to-cell junctions. *In* Methods in Membrane Biology. E. Korn, editor. Plenum Publishing Corp., New York. 10:121–434.

5. Johnston, M. F., and F. Ramon. 1982. Voltage independence of an electrotonic synapse. *Biophys. J.* 39:115–117.
6. Rall, W. 1977. Core conductor theory and cable properties of neurons. *In* Handbook of Physiology. The Nervous System. E. Kandel, editor. American Physiological Society, Bethesda, Maryland. 1(1,pt 1):33–97.
7. Spray, D. C., L. Harris, and M. V. L. Bennett. 1981. Equilibrium properties of voltage dependent junctional conductance. *J. Gen. Physiol.* 77:77–83.
8. Johnston, M. F, and F. Ramon. 1981. Electronic coupling in internally perfused crayfish segmented axons. *J. Physiol.* (*Lond.*). 317:509–518.
9. Perrachia, C. 1973. Low resistance junctions in crayfish. I. Two arrays of globules in junctional membranes. *J. Cell Biol.* 57:54–65.
10. Socolar, S. J., B. Rose, and A. L. Obaid. 1983. Control of cell-to-cell channel conductance in *Chironomus* salivary gland cells by cell membrane potentials: two independently regulated gates in series. *Biophys. J.* 41(2,Pt.2):217 *a*. (Abstr.)
11. Loewenstein, W. R. 1981. Junctional intercellular communication: the cell-to-cell membrane channel. *Physiol. Rev.* 61:829–913.